

UNIVERSIDADE FEDERAL DO RIO GRANDE DO SUL
INSTITUTO DE INFORMÁTICA
CURSO DE CIÊNCIA DA COMPUTAÇÃO

ARTHUR ENDRES BALBÃO

A Biologically Inspired Hair Aging Model

Work presented in partial fulfillment
of the requirements for the degree of
Bachelor in Computer Science

Advisor: Prof. Dr. Marcelo Walter

Porto Alegre
November 2021

UNIVERSIDADE FEDERAL DO RIO GRANDE DO SUL

Reitor: Prof. Carlos André Bulhões Mendes

Vice-Reitora: Prof^a. Patricia Pranke

Pró-Reitora de Graduação: Prof^a. Cíntia Inês Boll

Diretora do Instituto de Informática: Prof^a. Carla Maria Dal Sasso Freitas

Coordenador do Curso de Ciência de Computação: Prof. Rodrigo Machado

Bibliotecária-chefe do Instituto de Informática: Beatriz Regina Bastos Haro

ABSTRACT

Hair rendering has been a focal point of attention for the last couple of decades in computer graphics. However, there have been few contributions to the modeling and rendering of the natural hair aging phenomenon. Therefore, this work presents a new technique that simulates the process of hair greying on digital models. Our system is biologically inspired, supports facial hair, both genders, any ethnicity and is compatible with different lengths of hair strands. Our system is implemented on the graphics engine Unreal Engine 4, integrated with the MetaHuman framework. Our real-time results resemble real-life greying, which is accomplished by simulating the stochastic nature of the process and the gradual decay of melanin.

Keywords: Computer Graphics. Rendering. Hair greying. Biologically inspired. Unreal Engine 4. MetaHumans.

Um Modelo De Envelhecimento De Cabelos Inspirado Pela Biologia

RESUMO

Renderização de cabelos têm sido um grande foco da computação gráfica nas últimas décadas. Entretanto, existem apenas poucas contribuições no contexto de modelagem e renderização do fenômeno natural de envelhecimento capilar. Dessa forma, este trabalho apresenta uma nova técnica que busca simular o processo de envelhecimento do couro cabeludo em modelos digitais. Nosso sistema é inspirado pela biologia, suporta pelos faciais, ambos os gêneros, qualquer etnia e é compatível com diferentes comprimentos de folículos capilares. O nosso modelo é implementado no motor gráfico Unreal Engine 4, sendo integrado ao framework MetaHuman. Nossos resultados em tempo real são similares ao fenômeno de envelhecimento capilar na vida real, o que é alcançado através da simulação da natureza estocástica do processo e do decaimento gradual de melanina.

Palavras-chave: Envelhecimento de cabelo. Inspirado pela biologia. Unreal Engine 4. MetaHumans.

LIST OF FIGURES

Figure 1.1 Example of hair greying simulation enabled by our system. From left to right and top to down, the hairs progressively lose more melanin, thus becoming almost completely unpigmented at the end of the process.	11
Figure 2.1 Microscopic images of scalp hairs showing the absence of melanin on white hairs.	12
Figure 2.2 Regions of the hair scalp.....	13
Figure 2.3 Greying reversal in hair shaft.....	14
Figure 2.4 Individual hairs shown as lines, depicting its trajetories throughout the evolution of the model in time. Once the aging factor crosses a threshold, the hair no longer grows with its natural color, as it can be seen on the detailed view of a hair follicle on the left.	15
Figure 2.5 MetaHuman Creator User Interface.....	17
Figure 3.1 Automatic Face Aging using GANs	18
Figure 3.2 Real-time hair rendering using neural networks.....	19
Figure 3.3 Hair aging in The Irishman.....	20
Figure 3.4 Dynamic hair aging system	21
Figure 4.1 Overview of our pipeline	22
Figure 4.2 Normal vectors from the average planes of the head.....	23
Figure 5.1 This toy example shows an unwrapped texture of the model's head in a). This texture is then used as a color to shade the model in b) and as the hair color in c). As the hair is long and pulled back, the colors do not exactly match with what is seen on the naked head. Instead, each hair strand has its color defined by what color was assigned to its root, which indexes the texture through the Root UV node.	27
Figure 5.2 Image a) represents the normal map baked in Maya, where each texel represents a normal direction on the surface of the head. Image b) is the final output of K-Means, and c) the texture applied on our model's face.....	28
Figure 5.3 Each pixel in a) represents a follicle on the surface of the head. The images in b) are the binary masks obtained in our segmentation process. If we multiply the Follicle Texture in a) by each image in b), we will have the number of follicles in each area.	29
Figure 5.4 Image a) depicts a comparison between a simulation run with the original parameters, in blue, and one using the distinct values for specific hair regions, in orange. As it can be seen, there is no significant difference between the two models. As for b), it displays the aging disparity in each region, as the temples, occipital and the rest of the scalp reach 50% of grey hairs at, respectively, 74, 80 and 78 years of age.	32
Figure 5.5 Image a) shows a texture filled with b_0 parameters, which looks like a standard noise pattern. This is because we sample all the values from the same distribution with $\sigma_0 = 10$. As for Image b), the texture is filled with parameters for b_1 . We can clearly see the difference around the temporal region, which is closely situated to the ears of the subject. As the standard deviation is higher for this area, the region looks noticeably brighter. Both images were edited to provide a better viewing experience, once the original pixel values were much darker.	33

Figure 5.6 The picture depicts the depigmentation process occurring in a gradual fashion. From left to right, the melanin decreases along the hair shaft, starting from the root and finally reaching the hair tip. At the same time, the reduction of melanin gets more pronounced as time goes by, completely removing the natural color of the hair at the end.	33
Figure 5.7 Picture a) shows the implementation of Equation 2.1 inside the Material Editor. The number sampled from each texture is multiplied by 255, once the values were compressed in the range 0 to 1. Image b) depicts the final part of the desaturation process, where the hair that crosses the threshold of 1920 has its melanin reduced. This melanin value is then used by the Hair Color node, whose output is converted into a Luminance value through the Desaturation Node, resulting in the final color.	34
Figure 6.1 In the comparison, our model is able to simulate the early greying of the temporal area, which is also done by the method of Volkmann and Walter (2020). However, the model in c) does have a visible seam on the temples at the point where the grey hairs end. As seen on the reference in d), the greying of this area is not uniform, but stochastic. The pepper-and-salt system in b) manages to preserve the heterogeneity of the process, but does not account for the different rates of greying in each region.	35
Figure 6.2 The observations made in Figure 6.1 are even more pronounced in this picture, as the seam in the temporal region in c) becomes more noticeable. At the same time, the salt-and-pepper system from b) does not have a majority of grey or white hairs in the temples, as seen on the reference in d) or in our model in a).	36
Figure 6.3 The picture in the right depicts a man at 38 years of age, with no signs of hair greying. Our model, in the left and in the middle, has the same appearance at the age of 38, not showing any traces of grey hairs.	37
Figure 6.4 As the individual ages to 44 years, some grey hairs are now visible on the temporal region. Our model produces a similar result at the age of 58 years, where the hairs at the temples mostly consist of grey shafts.	37
Figure 6.5 At 55 years of age, the man's hair has a majority of grey follicles and shows even less pigmentation at the temporal areas. Our simulation presents a similar result at the age of 70, where most of the hairs have lost its original pigmentation and are now grey.	38
Figure 6.6 Now at 60 years old, the hair shafts that were grey in Figure 6.5 are now transitioning to a more unpigmented state, presenting a brighter tonality. Our model displays the same pattern at around 78 years. However, as the real-life subject is under warmer lighting conditions than those of our simulation, the visual comparison is not ideal. For this reason, we provide another comparison in the bottom row, where the temperature for our virtual light sources is defined as 5000K.	39
Figure 6.7 At 71 years of age, the man's hair is almost completely white, which is also shared by the hairs on the eyebrows. In our simulation, the 3D character exhibits a similar appearance at 90 years of age. Just like in Figure 6.6, we present another comparison in the bottom row, as the real-life picture was taken under warmer lighting conditions.	40

Figure 6.8 The figure shows a comparison between our visual simulation and the classification system suggested by Pospiech et al. (2020). As it can be seen, our simulation follows the pattern suggested in each category. However, there are some differences in the tonality of grey and white hairs, specially for Category 5 and 6. For Category 5, we believe that it could be a matter of lighting conditions and hairstyling. Where the real-life subject has short straight hair, our 3D character has a more voluminous curly hair, which results in more self-shadowing. As for Category 6, we believe that the yellowing of the subject's hair could be caused by photodegradation (RICHENA et al., 2014).	41
Figure 6.9 The images depict the generality of our system, which can be used with short and straight hair, such as in the first row, but also with Afro hair, in the third row, or long and curly hair, in the fifth row. The individual video for the female subject shows how the first area to be affected by greying is the top of the head, opposed to the temporal region in men.	42

LIST OF ABBREVIATIONS AND ACRONYMS

UE4	Unreal Engine 4
HF	Hair Follicle
HLSL	High-Level Shading Language
VRAM	Video Random Access Memory

CONTENTS

1 INTRODUCTION.....	10
2 BACKGROUND.....	12
2.1 Biological Background.....	12
2.2 Unreal Engine.....	16
2.3 MetaHumans	17
3 RELATED WORK	18
3.1 Face Aging	18
3.2 Hair Rendering.....	19
3.3 Hair aging systems	19
4 METHODOLOGY	22
4.1 Overview of our system	22
4.2 Preprocessing.....	23
4.2.1 Segmentation.....	23
4.2.2 Offline greying simulation	24
4.3 Visual Simulation	25
5 IMPLEMENTATION	27
5.1 Segmentation of the Hair Scalp	27
5.2 Offline Simulation	28
5.3 Visual Simulation	30
6 RESULTS.....	35
6.1 State-of-the-art	35
6.2 Real-Life Comparisons.....	36
6.3 Results with different hairstyles	38
7 CONCLUSION	43
REFERENCES.....	44

1 INTRODUCTION

Throughout the history of computer graphics, many contributions have been made in order to best model and render a human being in a digital world (IGARASHI; NISHINO; NAYAR, 2007; WARD et al., 2007; LEE et al., 2012). From animations to games, the subject has attracted the interest of both the academy and the industry in an endeavor to enable the production of photorealistic digital humans. One of the most complex challenges is the representation of realistic hair due to its complex geometry and the underlying interactions of light, resulting in subsurface scattering and self-shadowing. Although many advancements were made on shading (ZINKE et al., 2008; CHIANG et al., 2016) and the polygonal representation of hair (PETROVIC; HENNE; ANDERSON, 2005; JANSSON et al., 2019), the issue of hair graying in digital assets and how to accurately simulate the decay of melanin through time is currently not addressed.

Hence, this work presents a method for properly simulating the process of hair aging in digital humans. Our main contribution is a model for hair greying that is biologically inspired, can be executed in real-time, and adapts to any hair style, as well as facial hair. Besides the expected application in games or in the movie industry, we believe our work can be of great assistance for biological research, providing a better visual understanding of the hair aging process for hypothesis testing.

The body of this work is divided into 7 chapters, where Chapter 2 lays out the necessary biological foundations of hair graying, as well as some background information regarding the technology used in our work. Chapter 3 discusses related contributions to the present work, while Chapter 4 introduces the biologically inspired computational model used in our simulation. The details of our implementation are described in Chapter 5, including an automatic technique for segmenting the head scalp in regions of interest. Chapter 6 presents a discussion of our results, and Chapter 7 provides our conclusions, limitations and some possible extensions of our work.

In Figure 1.1 we show a sequence of images simulating the graying of a subject in our system.

Figure 1.1: Example of hair greying simulation enabled by our system. From left to right and top to down, the hairs progressively lose more melanin, thus becoming almost completely unpigmented at the end of the process.



Source: Generated by the author.

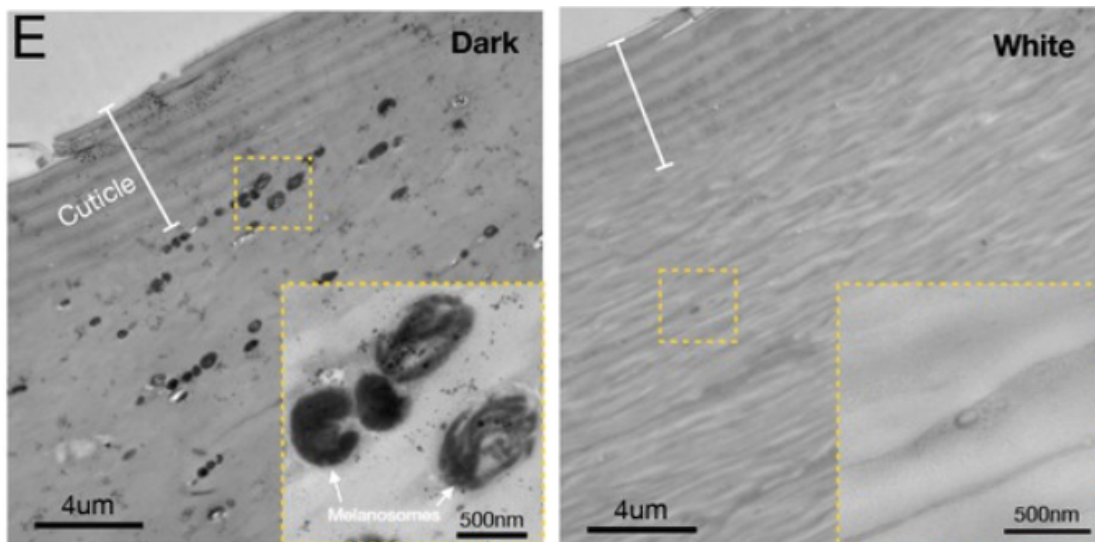
2 BACKGROUND

This chapter provides a biological background on hair aging, including characteristics across varying ages and different ethnic groups. In addition, we present a brief introduction to the technology used in our implementation.

2.1 Biological Background

From the appearance of wrinkles and dark spots on the face to changes in skin tone, the human body has several ways to convey the passage of time. One of its most prominent effects is hair greying, the phenomenon responsible for the loss of pigmentation in hair follicles. The hair aging process can be explained as the decrease in time in melanin granules' amount, size, and density. These melanin units, also known as melanosomes, are vital structures for the hair pigmentation mechanism. A comparison between melanosomes found in a dark, pigmented hair, and a white, unpigmented one, is shown in Figure 2.1.

Figure 2.1: Microscopic images of scalp hairs showing the absence of melanin on white hairs.



Source: Extracted from (ROSENBERG et al., 2021).

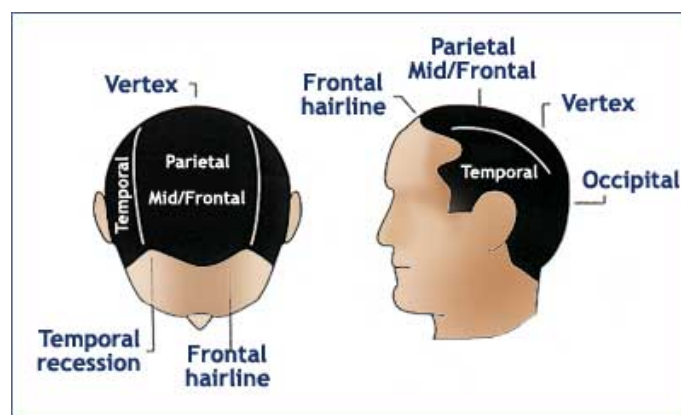
Despite an ongoing investigation of decades, there is no universally accepted model for hair greying (O'SULLIVAN et al., 2021). Nevertheless, many population studies (PANHARD; LOZANO; LOUSSOUARN, 2012; ACER et al., 2020; POSPIECH et

al., 2020) were conducted on the topic, shedding some light upon the phenomenon and its behavior across different ethnicities and phenotypes. It was believed (KEOGH; WALSH, 1965) that greying followed a 50/50/50 rule, which meant that, at 50 years of age, 50% of the population would have 50% of gray hairs. However, Panhard, Lozano and Lous-souarn (2012) revealed that only 6 to 23% of the population over 50 years old had 50% or more of grey hairs. In addition to that, the authors found that the presence and intensity of greying were dependent primarily on the ethnic, geographical origin, being the European/Caucasian group the most affected and the African-American/Sub-saharan African group the least.

It was also discovered that greying affects different regions of the hair scalp at different times across the lifespan of an individual. In order to discuss this topic, we would like to introduce the different areas of the head, which will be mentioned below. However, there does not seem to be an academic consensus on the names and boundaries of hair scalp regions. Therefore, we will be following the conventions used in Fig. 2.2.

It was observed in a group with ages between 45 and 65 years (PANHARD; LOZANO; LOUSSOUARN, 2012) that there was a disparity in the frequency of grey hairs throughout the hair scalp. In men, the temporal region had an incidence of 75% of grey hairs, compared to 67% on the vertex, and 58% on the occipital area. In women, the occipital area was also the least affected. However, both temporal and vertex regions showed similar values. According to Tobin (2008), in men, the temples are the first region to be affected, followed by greying on the vertex and then the remaining hairs of the scalp. At the same time, in women, the onset area of greying seems to be either the parietal region (ACER et al., 2020) or the frontal area (JO et al., 2012).

Figure 2.2: Regions of the hair scalp

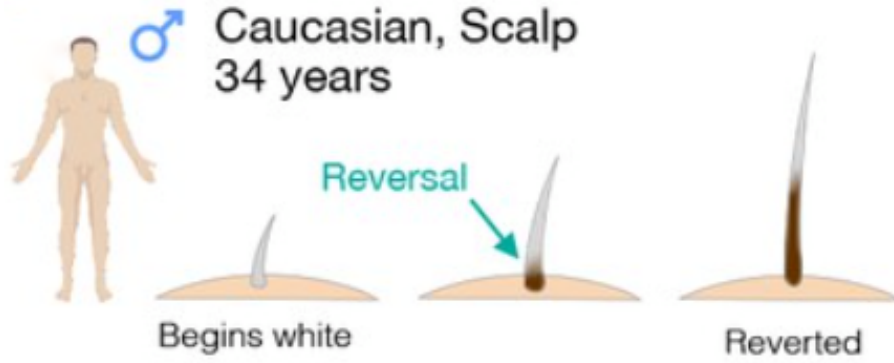


Source: <<https://www.hairtransplantmentor.com/htm-stagingfeb20/posterior-scalp/>>

Recently, Rosenberg et al. (2021) developed a new method for digitalizing hair shafts, allowing for a closer view of greying transitions across individual hair strands. With this new technology, they discovered that the greying process is reversible, at least temporarily. Depending on the amount of stress experienced by an individual, hair aging can be intensified. However, as soon as the stressful period ends, some hairs that began white can go through a repigmentation phase, starting to grow with their original color. In Figure 2.3 we show the greying reversal process.

In order to model hair greying, as well as the influence of stress on hair aging and the newly discovered phenomenon of greying reversal, a computational model was implemented. Their model will serve as a baseline to ours, a simplified version that does not account for the effects of stress.

Figure 2.3: Greying reversal in hair shaft



Source: Extracted from (ROSENBERG et al., 2021).

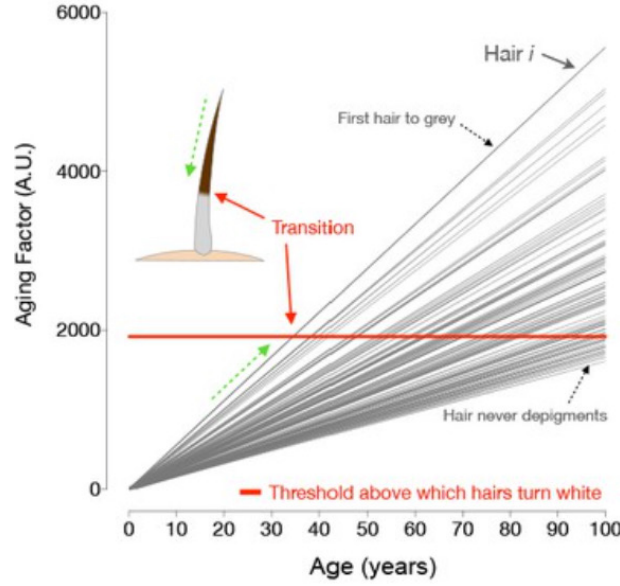
In the computational system described by Rosenberg et al. (2021), each hair has its own *Aging Factor* (AF), which can be interpreted as the age of each individual hair. As the *Aging Factor* crosses a certain threshold, the follicle loses its capacity to produce melanin, consequently turning white. This process is illustrated in Figure 2.4.

The *Aging Factor* for each hair is given by a linear mixed model, which supports both fixed and random effects to account for the stochastic nature of hair greying. The equation below represents the *Aging Factor* for a given i -th hair and a certain age in the simulation:

$$AgingFactor_{i,age} = |b_{0,i}| + (|b_{1,i}| + \beta_1) * age + (|b_{2,i}| + \beta_2) * AccumulatingStress_{age},$$

where $b_{0,i}$ is the initial aging factor, β_1 determines the aging factor rate and β_2 describes how sensitive is the aging factor to stressful events. The variables $b_{1,i}$ and $b_{2,i}$ add random

Figure 2.4: Individual hairs shown as lines, depicting its trajetories throughout the evolution of the model in time. Once the aging factor crosses a threshold, the hair no longer grows with its natural color, as it can be seen on the detailed view of a hair follicle on the left.



Source: Extracted from (ROSENBERG et al., 2021).

effects to, respectively, the aging factor rate and the sensitivity to stress for i -th hair. In order to ensure the positivity of the *Aging Factor*, only the absolute value of each effect is considered. Finally, $AccumulatingStress_{age}$ is described as:

$$AccumulatingStress_{age} = \sum_{a=age-WindowWidth}^{age} stress_a,$$

where *WindowWidth* imposes a limit on how much an earlier stressful event can influence the *Aging Factor* in the present. This way, only events that happened in the last *WindowWidth* years are relevant to the current moment in the simulation.

The random effects $b_{0,i}$, $b_{1,i}$ and $b_{2,i}$ follow a multivariate distribution as follows:

$$b_{0,i}, b_{1,i}, b_{2,i} \sim N(0, G),$$

where G is the covariance matrix:

$$G = \begin{bmatrix} \sigma_0^2 & \rho_{01}\sigma_0\sigma_1 & \rho_{02}\sigma_0\sigma_2 \\ \rho_{01}\sigma_1\sigma_0 & \sigma_1^2 & \rho_{12}\sigma_1\sigma_2 \\ \rho_{02}\sigma_2\sigma_0 & \rho_{12}\sigma_2\sigma_1 & \sigma_2^2 \end{bmatrix}$$

Considering that our work is solely focused on the hair simulation itself, and not on external factors such as stress, which is left as future work, we can simplify the linear mixed model to the following equation:

$$AgingFactor_{i,age} = |b_{0,i}| + (|b_{1,i}| + \beta_1) * age.$$

The computational model described above, although defining the aging factor carefully, does not model the different rates of greying across hair scalp regions, such as the early greying of the temporal area and the late greying of the occiput. Hence, we propose in Equation 2.1 a spatial-aware model that samples b_1 from j different distributions based on the hair regions.

$$AgingFactor_{i,age} = |b_{0,i}| + (|b_{1,i,j}| + \beta_1) * age. \quad (2.1)$$

2.2 Unreal Engine

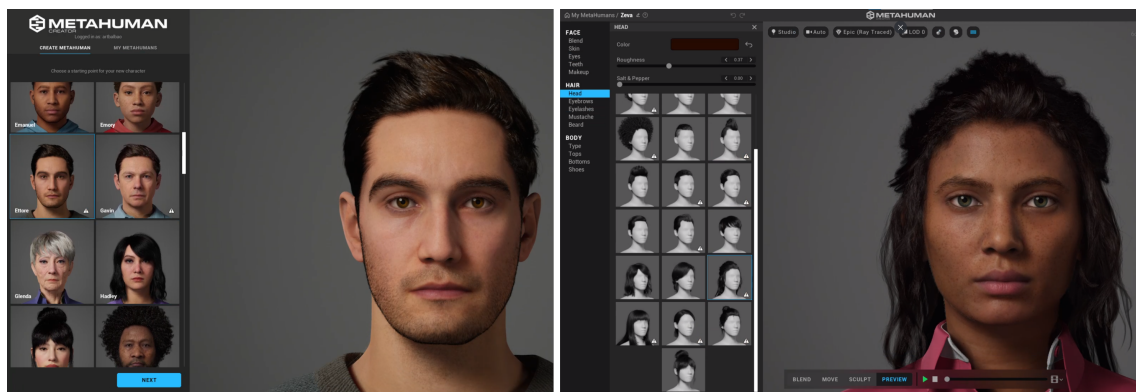
Unreal Engine 4 (Epic Games, 2014) is a popular game engine developed and maintained by Epic Games, currently on version 4.27.0. One of its defining features is called “Blueprint Scripting”, which can be thought of as a type of visual programming. In the system, each node corresponds to a module or function that receives a determined number of inputs, executes some code, and returns an output. Each node has to be connected to a previous node in order to execute. Hence, this flow mechanism functions very similar to a flowchart.

The appearance of an object is given by an asset called Material, which is controlled by the Material Editor. This interface can be seen as something very akin to Blueprint Scripting, in spite of the fact that its expressiveness is limited by HLSL code. Nevertheless, UE4 has a varied range of built-in material functions and nodes that can drastically reduce the amount of nodes needed in order to obtain some desired effect. A simple, yet very useful node for our project is the Desaturation Node, which converts a RGB vector into a luminance value, based on the defined contributions of each channel.

2.3 MetaHumans

MetaHuman Creator (Epic Games, 2021) is a cloud-based app, currently in a beta state of development, that allows users to create realistic models of human characters. As of today, it has more than 50 developed assets, which can be customized in many ways, from facial features to different body shapes and sizes. Once the user is satisfied with the resulting character, it can be easily exported to a vast range of 3d modeling software, such as Blender (Blender Foundation, 1994), Maya (Autodesk, Inc, 1999) and Cinema4D (MAXON Computer GmbH, 1991). However, only models exported to Unreal Engine are licensed to be published as final products. The user interface can be seen in Figure 2.5.

Figure 2.5: MetaHuman Creator User Interface



Source: Generated by the author.

In this chapter, we have provided the biological foundations that are necessary to better comprehend and reproduce the hair aging phenomenon. Also, we briefly introduced the technologies used in our work. In the next chapter, we will present papers that are related to our work, such as articles in Hair Rendering, as well as Face and Hair Aging.

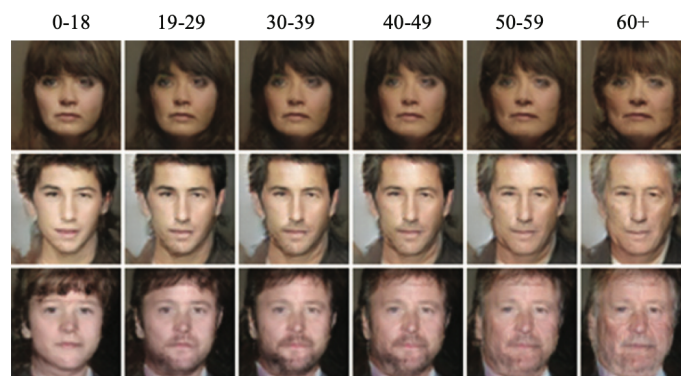
3 RELATED WORK

In this chapter, we discuss relevant papers in the context of our work, such as contributions in face aging, in addition to hair rendering and aging simulation systems.

3.1 Face Aging

The main goal of face aging is to produce a synthetic face image that looks either biologically younger or older than the original subject, while still trying to preserve the identity of the person. In this process, hair aging is just one of the components that needs to be addressed, as well as variations in skin tone, wrinkles, dark spots and other changes caused by the passing of time. Suo et al. (2010) models the aging process as a Markov chain, introducing a hierarchical And-Or graph structure that takes in consideration the many facial variations within an age group. Recently, Antipov, Baccouche and Dugelay (2017) presented a novel method that makes use of Generative Adversarial Networks (GANs) for automatic face aging. Some of their results are shown in Figure 3.1. As we can see, the hair greying phenomenon is simulated on the lateral areas of the head, as well as a visible receding hairline as age progresses. However, the images used in the technique have their upper boundaries matching the height of the hairline, as the method is mostly focused on face aging. Therefore, there is no information regarding hair greying across other areas of the hair scalp.

Figure 3.1: Automatic Face Aging using GANs



Source: Extracted from (ANTIPOV; BACCOUCHE; DUGELAY, 2017).

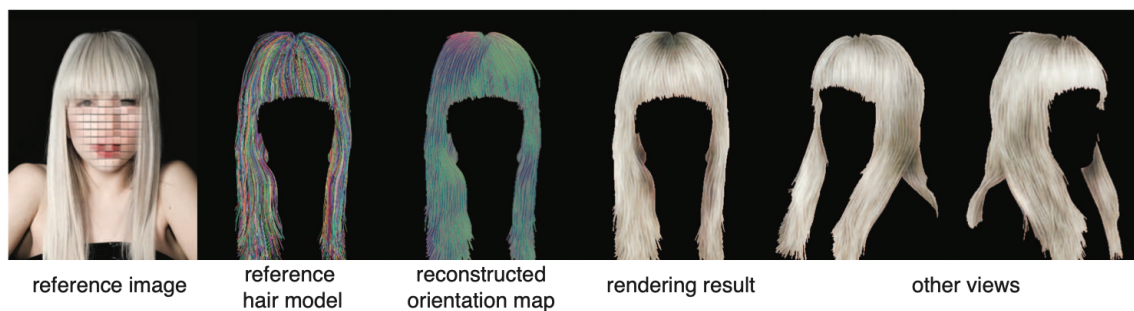
3.2 Hair Rendering

One of the most challenging elements to represent in a digital human is the hair scalp, due to the complexity of its geometry and the associated interactions of light, such as subsurface scattering and self-shadowing. In animation, the challenge of collision detection among individual strands is even harder. Nevertheless, this is a well established topic in the academy, and there are many techniques that focus on approximations to the light scattering phenomenon (ZINKE et al., 2008; YUKSEL; KEYSER, 2008; CHIANG et al., 2016).

Hair geometry has also been widely studied, and two models are most common in literature: volume (PETROVIC; HENNE; ANDERSON, 2005; XING et al., 2012) or explicit hair strands (YU et al., 2012; YUKSEL; TARIQ, 2010). Recent papers (ANDERSEN et al., 2016; LOUBET; NEYRET, 2017; JANSSON et al., 2019) have been exploring the possibility of combining both strategies, creating a hybrid model (JANSSON et al., 2019) that uses a strand-based system for closeups and a volumetric approximation for distant views.

Currently, there are also works on hair rendering using neural networks (WEI et al., 2018; SAITO et al., 2018), and results are shown on Figure 3.2.

Figure 3.2: Real-time hair rendering using neural networks



Source: Extracted from (WEI et al., 2018).

3.3 Hair aging systems

In the entertainment industry, many stories are centered around a character that ages throughout the narrative. Therefore, there is a need for, besides a face aging mechanism, a hair aging system that behaves realistically and can support the different transi-

tions that occur in the hair scalp across the lifespan of a human being.

Recently released, the feature film "The Irishman" (SCORSESE, M., 2019) is a biographical drama that follows the story of Frank Sheeran, a truck driver that becomes a hitman for the Italian Mafia. As the earlier moments are portrayed around 1950 and the later around the 2000s, Frank Sheeran, interpreted by Robert De Niro, needs to age accordingly. As De Niro himself was already 76 years old at the time of shooting, de-aging tools were specifically developed for the film. Frames from the picture displayed in Figure 3.3 show the amount of detail put in by the team at Industrial Light & Magic (ILM). The greying occurs in accordance with what is biologically known for men, that is, the first area to be affected is the temporal region (PANHARD; LOZANO; LOUSSOUARN, 2012). Unfortunately, there is little information about the nature of the hair aging system, and the different phases of greying seen in the movie could be the manual work of artists, not a dynamic aging system. However, as other characters also need to age in the film, a computational hair aging system would provide a more general, robust and biologically accurate solution.

Figure 3.3: Hair aging in The Irishman

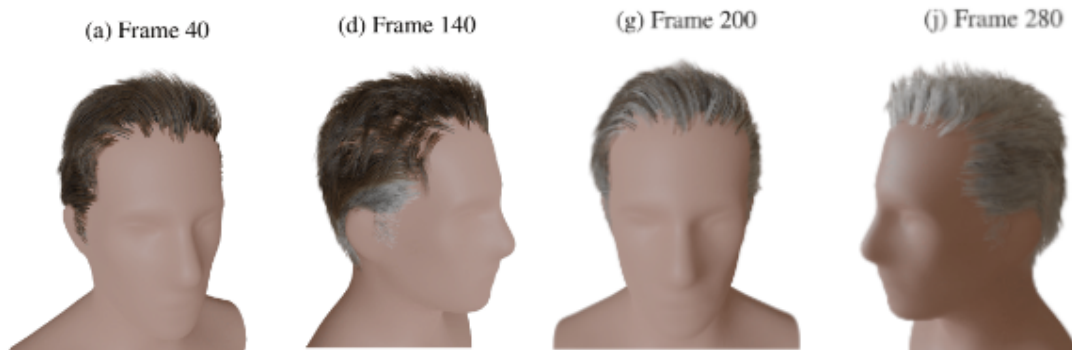


Source: Extracted from (SCORSESE, M., 2019).

There is only one known hair greying model (VOLKMANN; WALTER, 2020) in Computer Graphics, which describes a biologically-inspired aging system for male hair. The method, implemented in Blender, simulates the evolution of greying starting from the temporal region and spreading to the rest of the hair scalp in a later point of the process. In order to control this effect, the authors used manually segmented textures for the purpose of separating the different scalp regions. Due to the nature of the segmentation, there are visible seams along the different regions of the scalp as the aging advances. The work is also limited to males and does not generalize to different hairstyles, such as long hair.

The results of the simulation are shown in Figure 3.4.

Figure 3.4: Dynamic hair aging system



Source: Extracted from (VOLKMANN; WALTER, 2020).

In this chapter, we have presented related contributions to our work, such as papers in Face Aging, Hair Rendering and the state-of-the-art in Hair Aging. In the next chapter, we will expose the methodology behind our aging system, and Chapter 5 will describe the implementation-related aspects of the method.

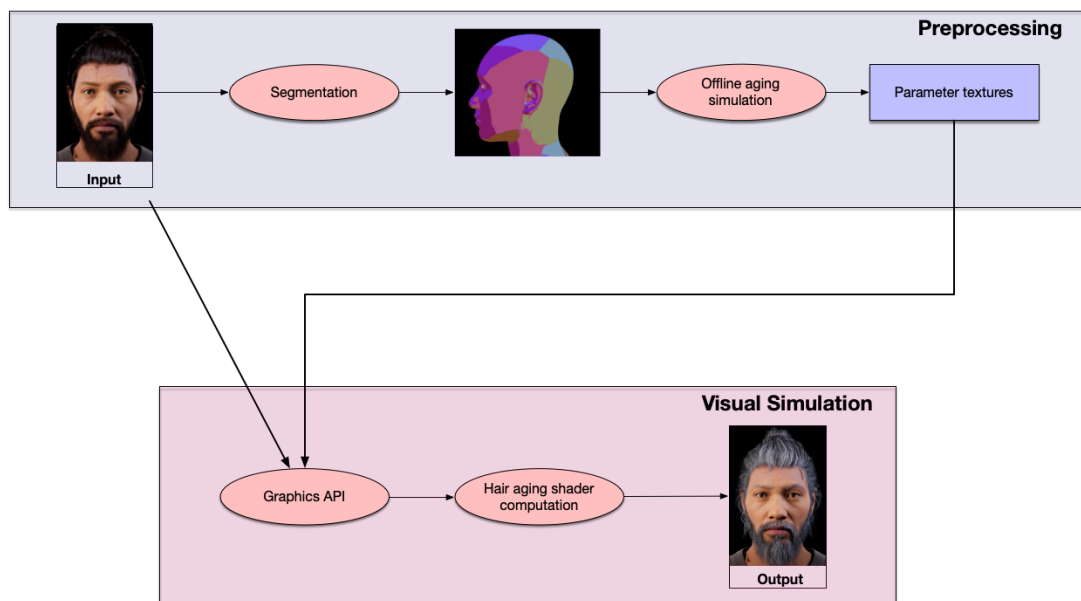
4 METHODOLOGY

This chapter explains the steps in our system without delving too deep into implementation details, which will be described in the following chapter. First, we present an overview of our pipeline, which is preceded by an exploration of the main ideas behind each step of our process.

4.1 Overview of our system

Our method consists of two separate parts: preprocessing and the actual visual simulation. In the preprocessing stage, the 3D character asset goes through a segmentation phase, where the head is divided in 5 different regions. Next, an offline aging model is used to define the distribution values that will be used for each hair follicle in our real-time simulation. These values are then saved in textures, having its texel coordinates attributed according to the segmentation masks. Lastly, the images are sampled and used during shader computations to render our hair aging simulation. An overview is shown in Figure 4.1.

Figure 4.1: Overview of our pipeline



Source: Generated by the author.

4.2 Preprocessing

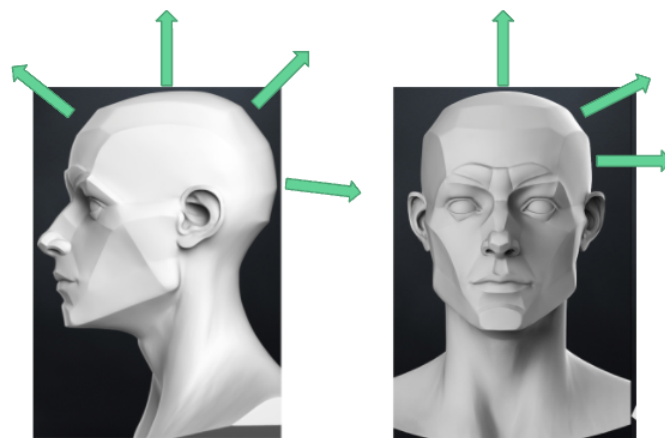
In this stage, we first compute a segmentation of the head to be used in the latter steps of our system. As the segmentation masks are computed, they will serve as input for our offline aging simulation, which will define the final parameter values for our visual simulation. As inputs for our model, we require the head mesh and its UV coordinates, which will be used to wrap our segmentation masks around the head.

This preprocessing step takes approximately 5 minutes to be completed, where most of the time is spent during the segmentation task, as the offline greying simulation only takes around 45 seconds to generate the final parameter values.

4.2.1 Segmentation

Graying occurs at different rates in different head parts. Therefore we need a way to compute these parts. Our key insight to enable an automatic segmentation is that each region of the head can be thought of as a plane whose normal vector is very distinct from other areas, as seen in Figure 4.2. Ergo, we can use clustering techniques to group normal vectors based on their orientation, thus defining regions by vectors similarity. In the next chapter we explain the use of K-Means Clustering for this task.

Figure 4.2: Normal vectors from the average planes of the head.



Source: <https://www.cgtrader.com/3d-print-models/art/sculptures/planes-of-the-head-male>.

4.2.2 Offline greying simulation

With our aging model defined in Equation 2.1, we have to set the possible values for β_1 , b_0 and b_1 . Based on data from Panhard, Lozano and Loussouarn (2012), where the first grey hairs appear on average at 35 years old, and at 65 years old the incidence of white hairs is close to 40%, Rosenberg et al. (2021) defined default parameter values that could describe the greying process of an average greyer. These values are displayed below, in Table 4.1.

Table 4.1: Default parameters for an average greyer, where σ_0 and σ_1 are standard deviations for, respectively, b_0 and b_1 .

<i>Parameter</i>	<i>Value</i>
β_1	16
σ_0	10
σ_1	13
Threshold	1920

Source: Rosenberg et al. (2021).

These parameters, defined for an average greyer, will serve as a baseline to our model, with β_1 set as 16 and b_0 centered at 0 with a standard deviation of 10. Nevertheless, as we defined in Equation 2.1, we would like to use different values for the standard deviation of b_1 to accelerate or postpone the greying on a determined region of the hair scalp. This is also the same parameter that is changed by Rosenberg et al. (2021) to model someone whose hair ages slower or faster than average. To account for these variations, the authors defined $\sigma_1 = 25$ for an early greyer and $\sigma_1 = 8$ for a late greyer.

There is no available data comparing the specific rates of greying on different hair zones throughout the lifespan of a person. To keep our model as accurate as we could to the phenomenon, we adopted a global rate of greying. That is, as long as the overall number of white hairs in the hair scalp is consistent with data obtained from the simulation from Rosenberg et al. (2021), the percentage of grey hairs in each region can be different without incurring in loss of fidelity to the original simulation. Thus, we sample b_1 from distributions which would provide convincing visuals in each region, while still maintaining a global accuracy to the computational model of Rosenberg et al. (2021).

In order to fine-tune the values for b_1 in each hair region while still conforming with the global rate of greying, we will be using an offline aging simulation, which takes as input the segmentation masks obtained in the previous step. In addition to that, it is also necessary to provide the amount of hair follicles in each hair region. That is because

our 3D models do not have the exact same number of hair follicles in the same area of the hair scalp. This is an impactful property in our simulation, since changing the values for one region will produce different outcomes for different assets.

For example, given two heads, A and B, where A has double the amount of HF that B has in the temporal region, and exactly the same number of hairs in other regions, we will need to use different distributions for the temporal areas of A and B. Otherwise, one of these models would have an incorrect global rate of greying.

Therefore, we propose a prior simulation, where, given the number of hairs in each area and the default values for b_0 and β_1 defined in Table 4.1, we test different possibilities of distributions for b_1 in each region. These results are then validated through our global rate of greying and saved to be used in the real-time model.

Also, the reasoning for specifically changing the standard values of b_1 for each hair region – and not β_1 or b_0 , which would also be viable options – is that since β_1 is a fixed value for all hairs, it does not need to be sampled from a texture. We can just assign it in the shader as a constant value. Therefore, if we were to give β_1 a different value for each hair region, we would need an extra image, resulting in more VRAM usage. For b_0 , as seen on Equation 2.1, the value is simply added to the total *Aging Factor*. As for b_1 , it is multiplied by the current year in the simulation. Therefore, b_1 can provide a more significant change in the total *Aging Factor* while having a smaller standard deviation. Consequently, this results in a smaller range of numbers to be fitted on an 8-bit texture.

4.3 Visual Simulation

As most of the work is done during the preprocessing stage, visual simulation of hair graying is performed in real-time. We just compute Equation 2.1 during shading time for each hair follicle. The parameters b_0 and b_1 are sampled from the textures generated in the offline simulation, and the threshold number and β_1 are constants given in Table 4.1.

As the aging factor for each hair crosses the threshold, the amount of melanin in the follicle starts to decrease. To control the decay rate, we calculate the time that has passed since crossing the threshold, which is defined in the Equation 4.1 for the i -th hair in the j -th hair region:

$$TimePastThreshold_{i,j} = \frac{AgingFactor_{i,j} - ThresholdValue}{|b_{1,i,j}| + \beta_1}. \quad (4.1)$$

The resulting value is represented in years, as $|b_{1,i,j}| + \beta_1$ describes how much the *Aging Factor* increases in a year, from Equation 2.1. This value is then divided by the number of years required for the melanin to reach its final amount. This will give us a number in the $[0,1]$ interval, which is used to interpolate between an upper and a lower bound of melanin.

Finally, we have to simulate the visual effect of the melanin decay spreading throughout the hair shaft, starting from the root and reaching the hair tip, as seen on the upper left side of Figure 2.4. We simulate this effect as follows. For a given point in the strand, we desaturate the natural color if enough time has passed for the unpigmented part to reach the length of the current point in the strand, starting from the moment the hair crosses the threshold.

However, this makes it necessary to know the growth rate for a hair strand in a year. LeBeau, Montgomery and Brewer (2011) define this number as 1 cm/month, or 12 cm/year. Therefore, we can describe the condition as:

$$DecayCondition = \begin{cases} yes, & \text{if } \frac{HairLength}{TimePastThreshold * YearlyGrowth} < 1 \\ no, & \text{otherwise,} \end{cases}$$

where *HairLength*, in cm, is defined as the current length of the hair shaft at the shading point and *Yearly Growth*, as mentioned earlier, is 12cm/year. *TimePastThreshold* is represented in years, and *DecayCondition* indicates whether the current point on the strand should have its melanin amount decreased.

This chapter presented an overview of the steps that were taken to produce a visual model for hair greying, from preprocessing to the actual real-time simulation. The next chapter will describe the aspects surrounding its implementation, and Chapter 6 will discuss the results obtained with our method.

5 IMPLEMENTATION

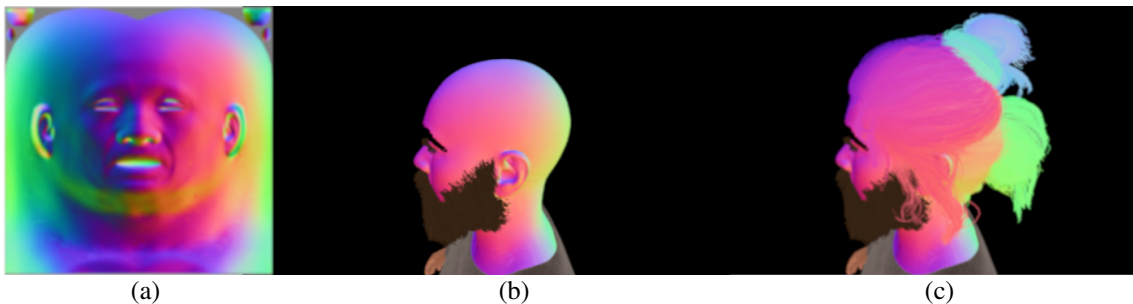
In this chapter, we describe the implementation aspects of our method, starting with a technique for segmenting the head scalp in regions of interest. From this point, we will obtain the number of hair follicles in each area of the scalp, which is a required input for our offline greying simulation. Finally, we will discuss how to incorporate the outputs from the model in a graphics pipeline such as Unreal Engine 4.

5.1 Segmentation of the Hair Scalp

The determinant factor for predicting the rate of greying of a specific follicle is the location of its root on the head. Therefore, to produce a robust segmentation that adapts to different hairstyles, such as long hair, we need to use this location as the segmentation criteria, that is, mapping the roots of each hair follicle to a location on the head.

Unreal Engine 4 has a feature called Root UV. This node carries the specific UV coordinates of the head where the hair root is located on. Therefore, we can apply the segmentation to a texture that is wrapped around the head mesh, and access this information via the Root UV node at any given point on the hair shaft. An exemplification of this mechanism is displayed in Fig. 5.1.

Figure 5.1: This toy example shows an unwrapped texture of the model's head in a). This texture is then used as a color to shade the model in b) and as the hair color in c). As the hair is long and pulled back, the colors do not exactly match with what is seen on the naked head. Instead, each hair strand has its color defined by what color was assigned to its root, which indexes the texture through the Root UV node.



Source: Generated by the author.

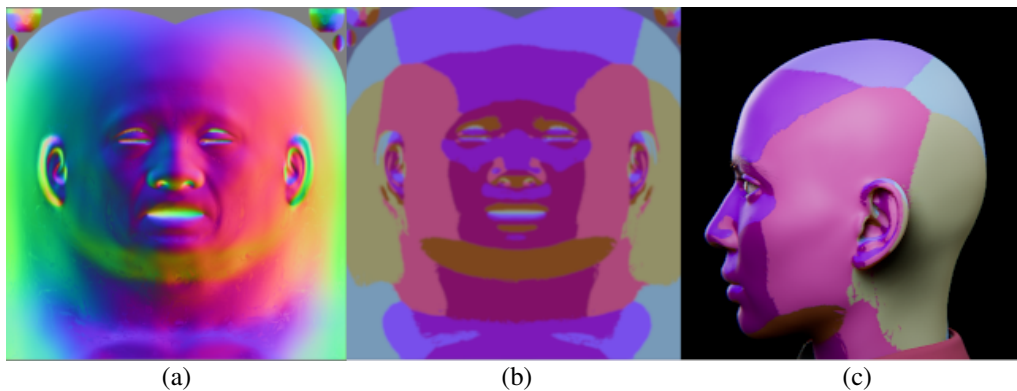
As we are interested in separating regions based on normals, represented as pixel values, we can apply a clustering method for aggregating pixels with similar colors, where

the RGB dimensions represent the XYZ normal directions.

To create a mapping of these normal vectors to a 2D representation, we can bake a normal map of the model's head in a 3D modelling software, given its UV coordinates. As the segmentation happens in the same image space, our segmentation masks will inherently be textures wrapped around the model's head. For that purpose, we use Maya (Autodesk, Inc, 1999) to bake our image containing the normal directions in each point of the head.

Finally, we aggregate the normals in groups through OpenCV's implementation of K-Means Clustering in Python 3.6, with K defined as 8 and the initialization algorithm of Arthur and Vassilvitskii (2007). Although we were only concerned with 5 areas, shown in Figure 2.2, we found it necessary to set K to 8 since our input image also contained data from the face and part of the neck, which are surfaces with different orientations. Therefore, they must be taken into consideration in our process. The method is illustrated in Figure 5.2. As we can see, the final mapping segments the desired regions according to the anatomical areas of the head.

Figure 5.2: Image a) represents the normal map baked in Maya, where each texel represents a normal direction on the surface of the head. Image b) is the final output of K-Means, and c) the texture applied on our model's face.



Source: Generated by the author.

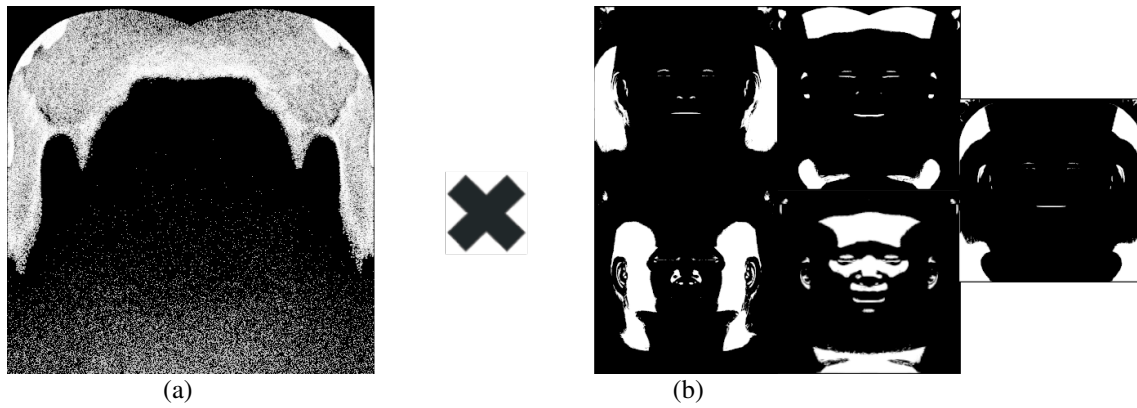
5.2 Offline Simulation

As discussed in Chapter 4, one of the required inputs for our offline simulation is the number of hair follicles in each region. This is necessary since the distribution of follicles on the hair scalp varies in each 3D asset, due to hairstyling and other factors.

Without this information, we would not be able to accurately establish a global rate of greying, and therefore, we wouldn't be able to compare the total number of white hairs in our simulation to the one presented in Rosenberg et al. (2021).

To calculate this number, we use our segmentation masks computed in the earlier steps, as long as we have a texture where the hair scalp is wrapped around the head mesh. Unreal Engine 4 provides this exact tool, which they call a "Follicle Texture". Its function is to project each follicle to a specific texel on the surface of the head. Hence, we can multiply this texture by each binary mask and sum the non zero pixels. This number will tell us the total amount of follicles per region. Figure 5.3 exemplifies the process.

Figure 5.3: Each pixel in a) represents a follicle on the surface of the head. The images in b) are the binary masks obtained in our segmentation process. If we multiply the Follicle Texture in a) by each image in b), we will have the number of follicles in each area.



Source: Generated by the author.

Finally, we can focus on finding good distributions for b_1 . This is a gender dependent issue, once male subjects will be affected by greying in a different way than women, as mentioned in Chapter 2. Therefore, for the sake of illustration, we will be using a male character from this point onwards, although the same process could be applied to a woman. In this case we would adjust the distributions for b_1 such that the parietal and frontal regions would have higher standard deviations, and consequently, would age faster than other areas of the scalp, as it is observed in women (ACER et al., 2020; JO et al., 2012).

From Panhard, Lozano and Loussouarn (2012), we know that men are, chronologically, first affected by greying in the temporal areas, followed by the top of the head, and last at the back of the head. Hence, we chose standard deviation values that would make the *Aging Factor* grow faster for the temples and slower in the nape area, while still

trying to remain close to the original greying rates from Rosenberg et al. (2021).

After applying the method for calculating the number of hairs per region to our subject, we found that its hair scalp had 20% of hair strands on the temporal region, 25% on the occipital area, and 55% on the remaining regions. Based on these percentages, we were able to define the standard deviations for each distribution as $\sigma_1 = 15$, $\sigma_1 = 12$ and $\sigma_1 = 13$ for respectively, the temporal area, the occipital region and the rest of the hair scalp. For the facial hair, we also set $\sigma_1 = 13$, as this region is usually first affected in a later time, according to Tobin (2008). The choice of 13 for most regions of the head is based on the fact that this is the same σ_1 used by Rosenberg et al. (2021) in their simulation. Therefore, we are, in fact, only changing the default value for areas that are noticeably more or less affected by greying. As seen in Figure 5.4, we are able to keep relatively close to the original global rate of greying, while still allowing for different rates in each region.

At last, we can fill the textures with values sampled from the distributions, as seen on Figure 5.5. For b_0 , which does not vary along the hair scalp, we can just sample from a distribution with $\sigma = 10$. For b_1 , we can use the binary masks from the segmentation stage to decide, for each texel, which distribution to sample from. For example, if the texel is located in the temporal region, we will sample from the distribution with the higher standard deviation of $\sigma = 15$. Each texture has a resolution of 2048x2048 to avoid aliasing artifacts.

5.3 Visual Simulation

To control the passing of time in our real-time simulation, we use the Timeline node available on UE4. Inside the node, the user can establish a period of time during which a variable will be interpolated between an initial and a final value. Hence, we can define an *age* variable that starts at 30 and ends at 100, within a period of 20 seconds. This way, each second in real life would be equivalent to 3.5 years in the simulation. The current value of the variable is then updated at every tick on a Material Collection instance, which can be accessed inside our Hair Material.

A neat consequence of this system is that we can easily revert the aging process using the Timeline node, which allows for time to be interpolated from the end of the defined period to its starting point. Therefore, besides aging, our implementation also supports real-time simulation of de-aging.

Inside the Material Editor, we sample the textures computed in the previous stage to obtain the correct distributions values. The UV coordinates used are the Root UV coordinates, as these textures are wrapped around the head of our subject. Finally, we can apply Equation 2.1 to obtain the *Aging Factor* for the current hair follicle.

When the *Aging Factor* crosses the threshold of 1920, as defined by Rosenberg et al. (2021), we must decide if the current shading point on the hair shaft should have its melanin decreased, as discussed in Chapter 4. We compute Equation 4.1, which gives us the time, in years, since the HF crossed the threshold. Unreal Engine provides us with the specific hair length at the shading point through the Hair Properties node. As the Yearly Growth for a hair strand is assumed to be 12 cm per year, we already know all the variables to calculate the condition for the melanin decay.

Finally, we control the decline in melanin through a linear interpolation between an upper and a lower bound:

$$melanin = LowerMelaninBound * \alpha + (1 - \alpha) * (UpperMelaninBound),$$

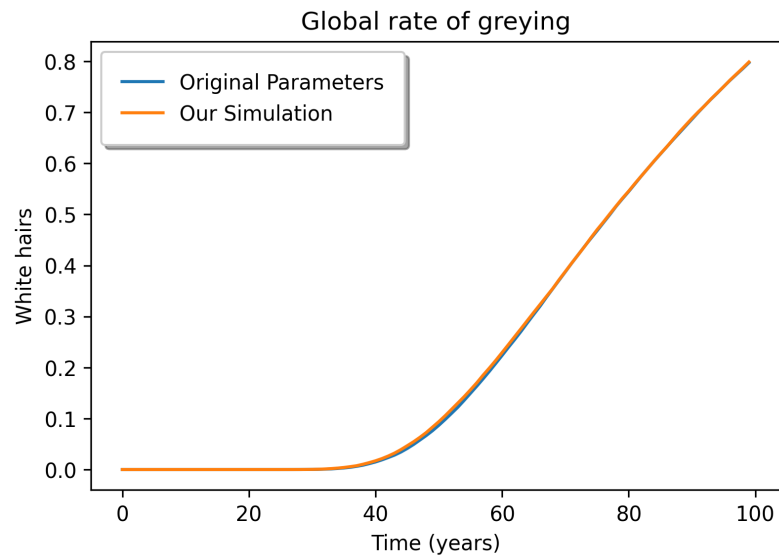
where the upper bound was experimentally defined as half the original amount of melanin, and the lower bound was set to 0.05, as less than this value resulted in a visually unappealing color. The value for α is computed through the equation below:

$$\alpha = \min\left(\frac{TimePastThreshold}{DesaturationTime}, 1\right),$$

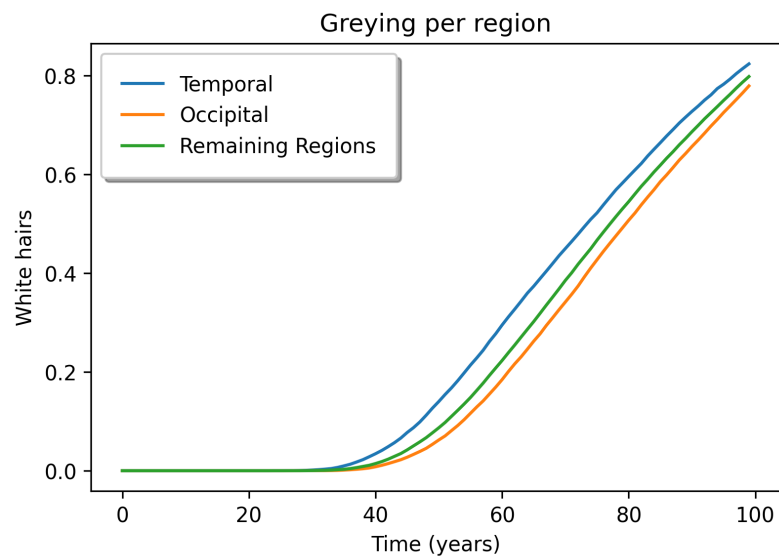
where *DesaturationTime* is a constant that tells us how many years does it take for the hair to reach the its final melanin value. We found through visual comparisons with real-life images that 20 years was a reasonable value for this decaying event. A visualization of these visual features is available in Figure 5.6. An overview of the process inside the Material Editor is seen in Figure 5.7.

In this chapter, we explained the most important aspects of our implementation, from details related to Unreal Engine, to the clustering method used in our segmentation and the visual effects of melanin decay in our real-time simulation. In the next chapter, we will present our results and comparisons with the state-of-the-art and real-life cases.

Figure 5.4: Image a) depicts a comparison between a simulation run with the original parameters, in blue, and one using the distinct values for specific hair regions, in orange. As it can be seen, there is no significant difference between the two models. As for b), it displays the aging disparity in each region, as the temples, occipital and the rest of the scalp reach 50% of grey hairs at, respectively, 74, 80 and 78 years of age.



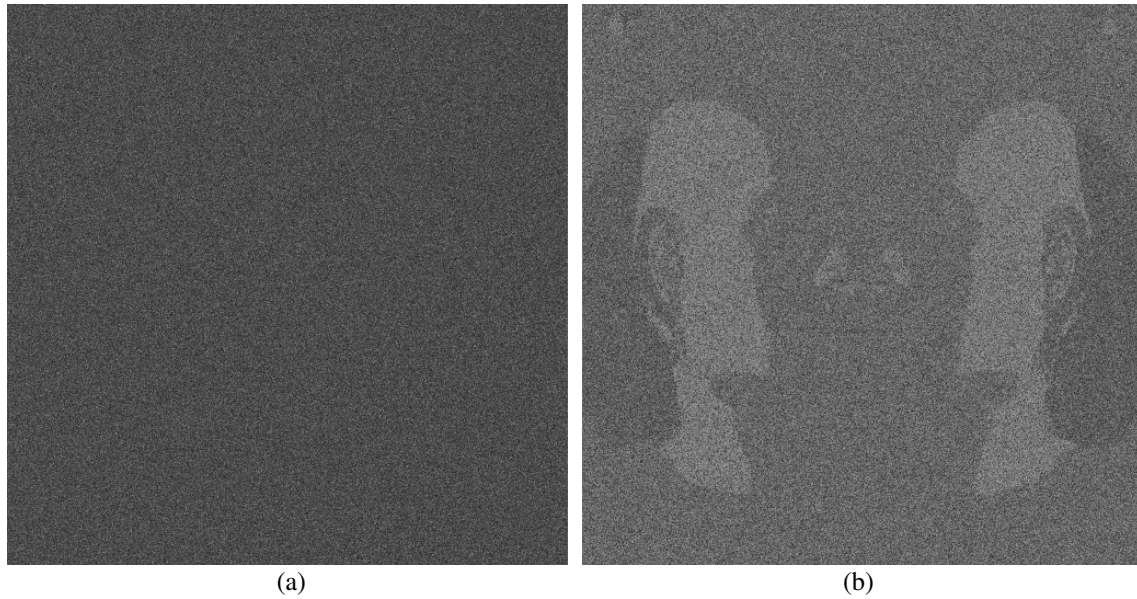
(a)



(b)

Source: Generated by the author.

Figure 5.5: Image a) shows a texture filled with b_0 parameters, which looks like a standard noise pattern. This is because we sample all the values from the same distribution with $\sigma_0 = 10$. As for Image b), the texture is filled with parameters for b_1 . We can clearly see the difference around the temporal region, which is closely situated to the ears of the subject. As the standard deviation is higher for this area, the region looks noticeably brighter. Both images were edited to provide a better viewing experience, once the original pixel values were much darker.



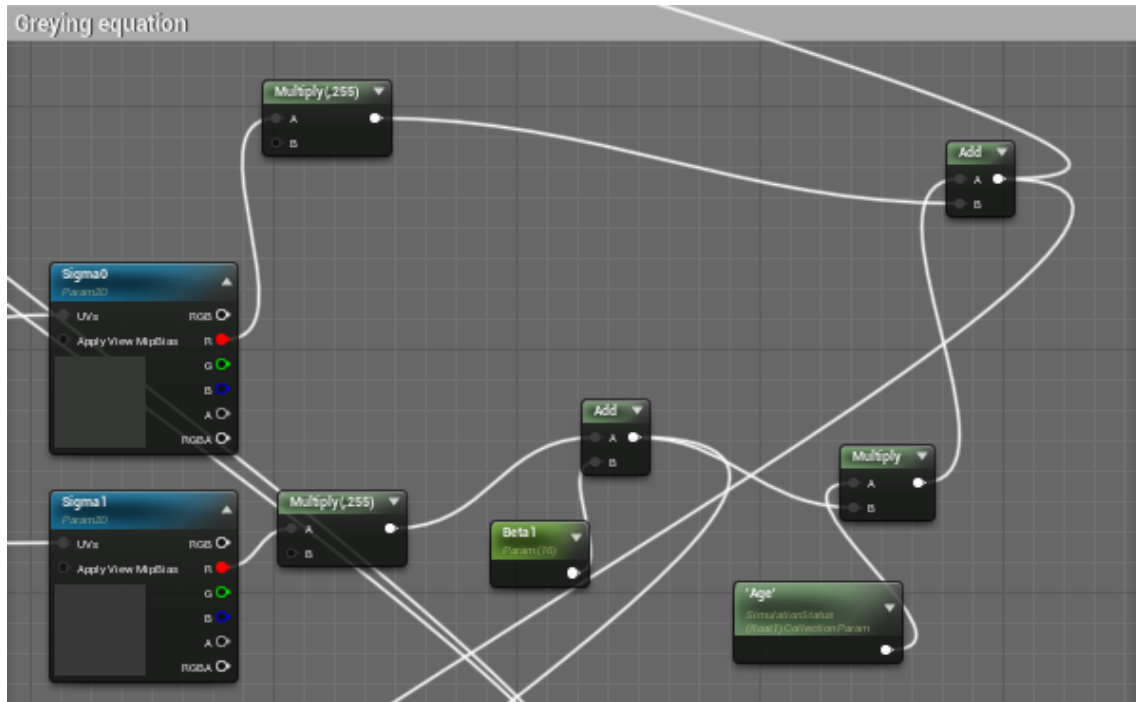
Source: Generated by the author.

Figure 5.6: The picture depicts the depigmentation process occurring in a gradual fashion. From left to right, the melanin decreases along the hair shaft, starting from the root and finally reaching the hair tip. At the same time, the reduction of melanin gets more pronounced as time goes by, completely removing the natural color of the hair at the end.

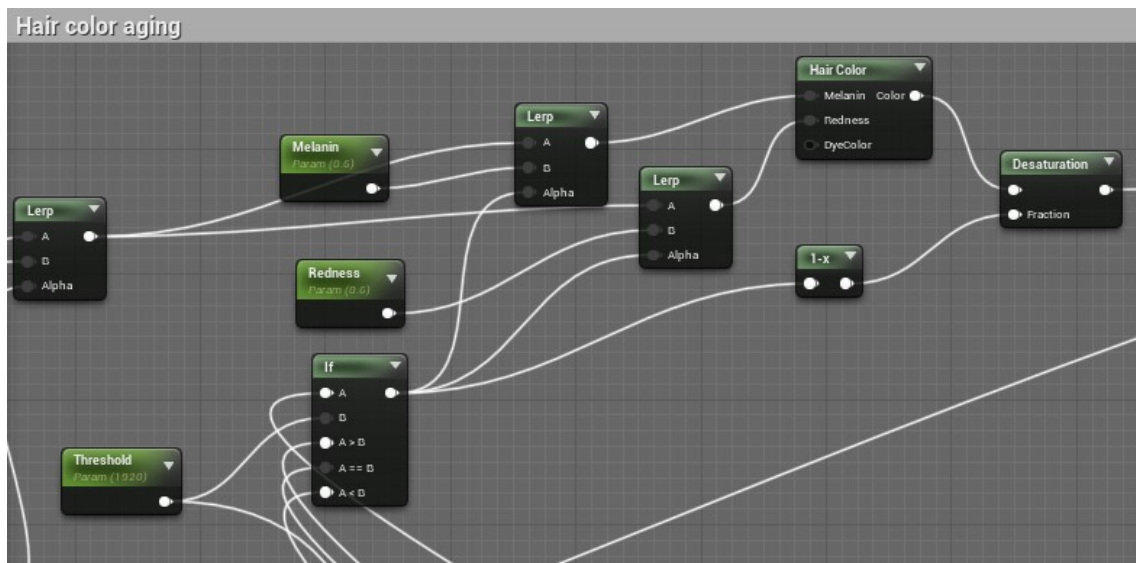


Source: Generated by the author.

Figure 5.7: Picture a) shows the implementation of Equation 2.1 inside the Material Editor. The number sampled from each texture is multiplied by 255, once the values were compressed in the range 0 to 1. Image b) depicts the final part of the desaturation process, where the hair that crosses the threshold of 1920 has its melanin reduced. This melanin value is then used by the Hair Color node, whose output is converted into a Luminance value through the Desaturation Node, resulting in the final color.



(a)



(b)

Source: Generated by the author.

6 RESULTS

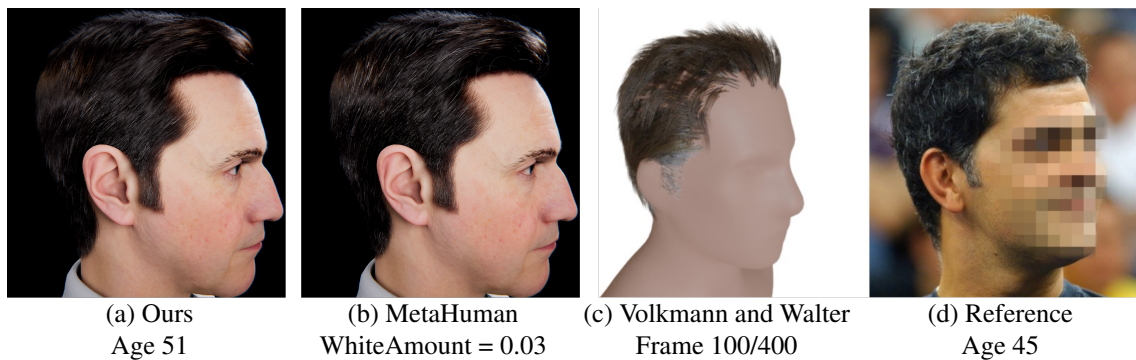
This chapter presents a discussion of the results obtained with our method. We start by comparing our work to the state-of-the-art in hair greying simulation, an area that is still mostly unexplored. For that reason, we also validate our results against real-life subjects. Finally, we assess the generality of our method by testing our system with different hairstyles.

Our tests were performed on an Intel i7 3770k @ 3.5 GHz paired with a NVIDIA RTX 2070 SUPER on Windows 10, averaging 45 FPS at 1920x1080, at "Cinematic Quality" settings in Unreal Engine 4.

6.1 State-of-the-art

In this section, we compare our work with the only known dynamic system for hair ageing (VOLKMANN; WALTER, 2020), as well as the solution implemented in MetaHuman Creator to simulate grey hairs, which uses salt-and-pepper noise to replicate the stochastic nature of greying.

Figure 6.1: In the comparison, our model is able to simulate the early greying of the temporal area, which is also done by the method of Volkmann and Walter (2020). However, the model in c) does have a visible seam on the temples at the point where the grey hairs end. As seen on the reference in d), the greying of this area is not uniform, but stochastic. The pepper-and-salt system in b) manages to preserve the heterogeneity of the process, but does not account for the different rates of greying in each region.

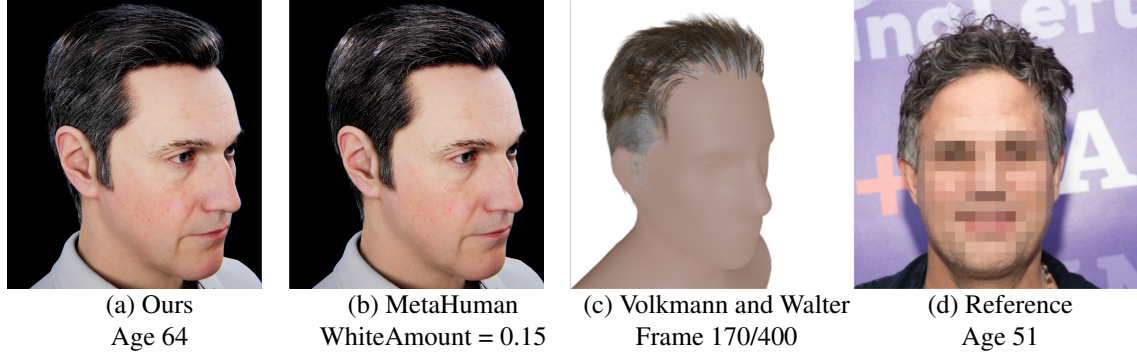


Source a) and b): Generated by the author.

Source c) and d): Extracted from (VOLKMANN; WALTER, 2020).

Their system can only be adjusted through a *WhiteAmount* slider that interpolates between 100% pepper - which would be fully pigmented, to 100% salt, or white hairs.

Figure 6.2: The observations made in Figure 6.1 are even more pronounced in this picture, as the seam in the temporal region in c) becomes more noticeable. At the same time, the salt-and-pepper system from b) does not have a majority of grey or white hairs in the temples, as seen on the reference in d) or in our model in a).



Source a) and b): Generated by the author.

Source c) and d): Extracted from (VOLKMANN; WALTER, 2020).

The effect is applied overall in all the hairs. Also, the method does not incorporate the notion of time, and can only be manually controlled by artists.

In Figures 6.1 and 6.2, we compare our work with the original results of Volkmann and Walter (2020), and tweak the salt-and-pepper values in MetaHuman Creator to render an image that resembles the reference picture. We recommend zooming in on the pictures in order to best visualize the effects.

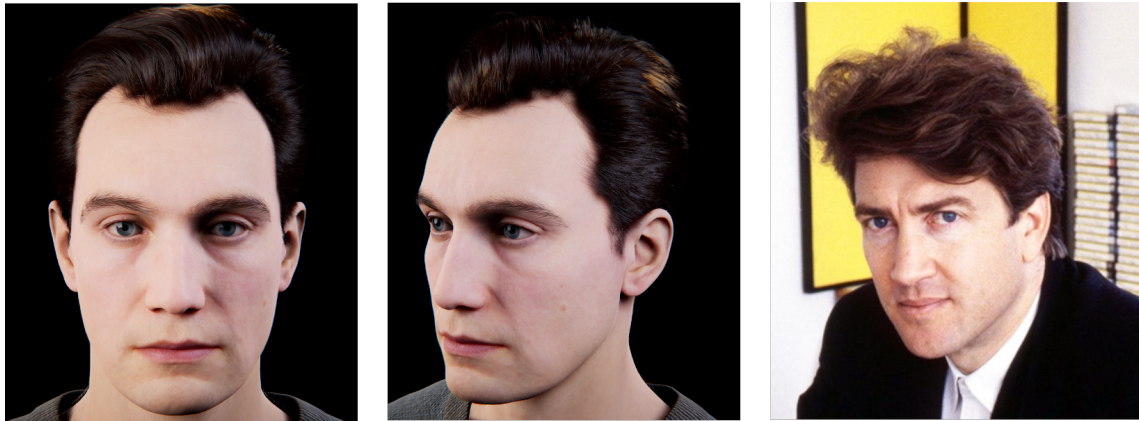
6.2 Real-Life Comparisons

As the state-of-the-art in this area is still incipient, we also compare our work to real-life subjects in order to validate our results. For this purpose, we will be using pictures taken throughout the life of a single person, as this will allow us to make a direct comparison between the evolution of our simulation and the progression of hair aging on a real individual.

However, our aging results may not be the best match of the subject's hair at the same instant in time. That is because our model is based on an average greyer, while the hair aging on the subject could be either slower or faster than average. For this reason, we will be selecting the moment in our simulation that best fits the real picture, based on a time window of 20 years around the person's age at the time of the photo. This age gap was chosen based on data from Rosenberg et al. (2021), where the onset age is

approximately 20, 40 and 50 years for, respectively, early, average and late greyers. The comparisons are shown in Figures 6.3 to 6.7.

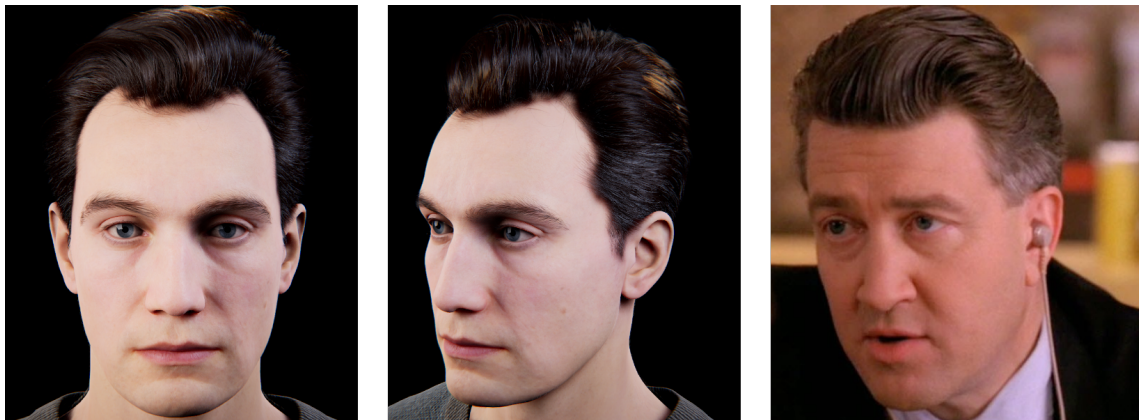
Figure 6.3: The picture in the right depicts a man at 38 years of age, with no signs of hair greying. Our model, in the left and in the middle, has the same appearance at the age of 38, not showing any traces of grey hairs.



Source left and middle: Generated by the author.

Source right: <<https://theacademy.tumblr.com/post/107272579301/david-lynch-1984>>

Figure 6.4: As the individual ages to 44 years, some grey hairs are now visible on the temporal region. Our model produces a similar result at the age of 58 years, where the hairs at the temples mostly consist of grey shafts.



Source left and middle: Generated by the author.

Source right:<<http://caveoftheflickeringlight.blogspot.com/2014/05/>>

In addition to that, we would also like to compare our results to the hair greying 6-stage classification system suggested by Pospiech et al. (2020), which is shown in Figure 6.8.

Figure 6.5: At 55 years of age, the man’s hair has a majority of grey follicles and shows even less pigmentation at the temporal areas. Our simulation presents a similar result at the age of 70, where most of the hairs have lost its original pigmentation and are now grey.



Source left and middle: Generated by the author.

Source right: <https://www.ilfattoquotidiano.it/2016/01/20/david-lynch-70-anni-e-mai-un-oscar-la-lunga-e-misteriosa-carriera-di-un-genio-del-grande-schermo/2389258/>

6.3 Results with different hairstyles

Finally, we show how our system can be used with a vast range of hairstyles and facial hair in Figure 6.9. A playlist with the complete simulation and different viewpoints for each subject is available at:

<https://youtube.com/playlist?list=PLm8DsMl5JjeMErn6GzNXDK3Ti0kZYM9kP>.

In this chapter, we have provided our visual results, proving that our system is capable of producing a realistic simulation of hair greying that can handle different types of hair and facial hair, while still maintaining a real-time framerate. In the next chapter, we will present our conclusions, the limitations of our work and what can be expected for future work.

Figure 6.6: Now at 60 years old, the hair shafts that were grey in Figure 6.5 are now transitioning to a more unpigmented state, presenting a brighter tonality. Our model displays the same pattern at around 78 years. However, as the real-life subject is under warmer lighting conditions than those of our simulation, the visual comparison is not ideal. For this reason, we provide another comparison in the bottom row, where the temperature for our virtual light sources is defined as 5000K.



Source left and middle: Generated by the author.

Source right: <https://www.imdb.com/name/nm0000186/mediaviewer/rm2687146752/?context=default>

Figure 6.7: At 71 years of age, the man's hair is almost completely white, which is also shared by the hairs on the eyebrows. In our simulation, the 3D character exhibits a similar appearance at 90 years of age. Just like in Figure 6.6, we present another comparison in the bottom row, as the real-life picture was taken under warmer lighting conditions.



Source left and middle: Generated by the author.

Source right: <https://www.imdb.com/name/nm0000186/mediaviewer/rm993929728/?context=default>

Figure 6.8: The figure shows a comparison between our visual simulation and the classification system suggested by Pospiech et al. (2020). As it can be seen, our simulation follows the pattern suggested in each category. However, there are some differences in the tonality of grey and white hairs, specially for Category 5 and 6. For Category 5, we believe that it could be a matter of lighting conditions and hairstyling. Where the real-life subject has short straight hair, our 3D character has a more voluminous curly hair, which results in more self-shadowing. As for Category 6, we believe that the yellowing of the subject's hair could be caused by photodegradation (RICHENA et al., 2014).



Source for Rows 1 and 3: Extracted from (POSPIECH et al., 2020). Source for Rows 2 and 4: Generated by the author.

Figure 6.9: The images depict the generality of our system, which can be used with short and straight hair, such as in the first row, but also with Afro hair, in the third row, or long and curly hair, in the fifth row. The individual video for the female subject shows how the first area to be affected by greying is the top of the head, opposed to the temporal region in men.



Source: Generated by the author.

7 CONCLUSION

We have presented a real-time solution for the simulation of the hair aging phenomenon. The system is biologically inspired, supports facial hair, both genders and any hairstyle. As our model does not require artistic input, we expect it can be used by the average user to age 3D characters in a convincing fashion. In addition to that, we believe our work can provide a visual aid to researchers in the dermatology field, which could use our model for hypothesis testing.

We developed our system based on data for an average greyer. Consequently, a person whose hair ages faster or slower than average may have a different appearance than the one provided by our model at the same age, as discussed in Chapter 6. Also, our model does not account for the ethnic origin of our character, a property that could influence the rate of greying, as presented by Panhard, Lozano and Loussouarn (2012).

Therefore, in future work, we plan to develop a framework that is more general, robust and supports multiple greying profiles - such as early, average and late, in addition to the geographical origin of our subject. Furthermore, we hope to incorporate external factors that can have a consequence on hair aging, such as stress, and the effect of greying reversal that is associated with it.

REFERENCES

ACER, E. et al. Clinical and epidemiological characteristics and associated factors of hair graying: a population-based, cross-sectional study in Turkey. v. 95, n. 4, p. 439–446, 2020. ISSN 1806-4841.

ANDERSEN, T. G. et al. Hybrid fur rendering: combining volumetric fur with explicit hair strands. v. 32, n. 6, p. 739–749, 2016. ISSN 1432-2315. Available from Internet: <<https://doi.org/10.1007/s00371-016-1252-x>>.

ANTIPOV, G.; BACCOUCHE, M.; DUGELAY, J.-L. **Face Aging With Conditional Generative Adversarial Networks**. 2017.

ARTHUR, D.; VASSILVITSKII, S. k-means++: the advantages of careful seeding. In: **Proceedings of the eighteenth annual ACM-SIAM symposium on Discrete algorithms**. [S.l.: s.n.], 2007. p. 1027–1035.

Autodesk, Inc. **Maya**. 1999. Available from Internet: <<https://www.autodesk.com/products/maya/>>.

Blender Foundation. **Blender**. 1994. Available from Internet: <<https://www.blender.org/>>.

CHIANG, M. et al. A practical and controllable hair and fur model for production path tracing. **Computer Graphics Forum**, v. 35, p. 275–283, 05 2016.

Epic Games. **Unreal Engine 4**. 2014. Available from Internet: <<https://www.unrealengine.com>>.

Epic Games. **MetaHuman Creator**. 2021. Available from Internet: <<https://metahuman.unrealengine.com/>>.

IGARASHI, T.; NISHINO, K.; NAYAR, S. K. **The Appearance of Human Skin: A Survey**. [S.l.: s.n.], 2007.

JANSSON, E. S. V. et al. Real-Time Hybrid Hair Rendering. In: BOUBEKEUR, T.; SEN, P. (Ed.). **Eurographics Symposium on Rendering - DL-only and Industry Track**. [S.l.]: The Eurographics Association, 2019. ISBN 978-3-03868-095-6. ISSN 1727-3463.

JO, S. J. et al. Hair graying pattern depends on gender, onset age and smoking habits. v. 92, n. 2, p. 160–161, 2012. ISSN 1651-2057.

KEOGH, E. V.; WALSH, R. J. Rate of Greying of Human Hair. Nature Publishing Group, v. 207, n. 4999, p. 877–878, 1965. ISSN 1476-4687. Available from Internet: <<https://www.nature.com/articles/207877a0>>.

LEBEAU, M. A.; MONTGOMERY, M. A.; BREWER, J. D. The role of variations in growth rate and sample collection on interpreting results of segmental analyses of hair. **Forensic Science International**, v. 210, n. 1, p. 110–116, 2011. ISSN 0379-0738. Available from Internet: <<https://www.sciencedirect.com/science/article/pii/S0379073811000776>>.

LEE, D. et al. Modeling and simulation of skeletal muscle for computer graphics: A survey. **Found. Trends. Comput. Graph. Vis.**, Now Publishers Inc., Hanover, MA, USA, v. 7, n. 4, p. 229–276, abr. 2012. ISSN 1572-2740. Available from Internet: <<https://doi.org/10.1561/06000000036>>.

LOUBET, G.; NEYRET, F. Hybrid mesh-volume LoDs for all-scale pre-filtering of complex 3D assets. v. 36, n. 2, p. 431–442, 2017. ISSN 1467-8659. Available from Internet: <<https://onlinelibrary.wiley.com/doi/abs/10.1111/cgf.13138>>.

MAXON Computer GmbH. **Cinema 4D**. 1991. Available from Internet: <<https://www.maxon.net/en/cinema-4d>>.

O'SULLIVAN, J. D. B. et al. The biology of human hair greying. v. 96, n. 1, p. 107–128, 2021. ISSN 1469-185X. Available from Internet: <<https://onlinelibrary.wiley.com/doi/abs/10.1111/brv.12648>>.

PANHARD, S.; LOZANO, I.; LOUSSOUARN, G. Greying of the human hair: a worldwide survey, revisiting the '50' rule of thumb. v. 167, n. 4, p. 865–873, 2012. ISSN 1365-2133. Available from Internet: <<https://onlinelibrary.wiley.com/doi/abs/10.1111/j.1365-2133.2012.11095.x>>.

PETROVIC, L.; HENNE, M.; ANDERSON, J. **Volumetric Methods for Simulation and Rendering of Hair**. 2005.

POSPIECH, E. et al. Exploring the possibility of predicting human head hair greying from DNA using whole-exome and targeted NGS data. v. 21, n. 1, p. 538, 2020. ISSN 1471-2164. Available from Internet: <<https://doi.org/10.1186/s12864-020-06926-y>>.

RICHENA, M. et al. Yellowing and bleaching of grey hair caused by photo and thermal degradation. **Journal of Photochemistry and Photobiology B: Biology**, v. 138, p. 172–181, 2014. ISSN 1011-1344. Available from Internet: <<https://www.sciencedirect.com/science/article/pii/S1011134414001857>>.

ROSENBERG, A. M. et al. Quantitative mapping of human hair greying and reversal in relation to life stress. **eLife**, eLife Sciences Publications, Ltd, v. 10, p. e67437, jun. 2021. ISSN 2050-084X. Available from Internet: <<https://doi.org/10.7554/eLife.67437>>.

SAITO, S. et al. 3d hair synthesis using volumetric variational autoencoders. **ACM Trans. Graph.**, Association for Computing Machinery, New York, NY, USA, v. 37, n. 6, dec. 2018. ISSN 0730-0301. Available from Internet: <<https://doi.org/10.1145/3272127.3275019>>.

SCORSESE, M. **The Irishman**. Netflix, 2019. Available from Internet: <<https://www.imdb.com/title/tt1302006/>>.

SUO, J. et al. A compositional and dynamic model for face aging. **IEEE Transactions on Pattern Analysis and Machine Intelligence**, v. 32, n. 3, p. 385–401, 2010.

TOBIN, D. J. Human hair pigmentation – biological aspects. **International Journal of Cosmetic Science**, v. 30, n. 4, p. 233–257, 2008. Available from Internet: <<https://onlinelibrary.wiley.com/doi/abs/10.1111/j.1468-2494.2008.00456.x>>.

VOLKMANN, D. V.; WALTER, M. A Practical Male Hair Aging Model. In: WILKIE, A.; BANTERLE, F. (Ed.). **Eurographics 2020 - Short Papers**. [S.l.]: The Eurographics Association, 2020. ISBN 978-3-03868-101-4. ISSN 1017-4656.

WARD, K. et al. A survey on hair modeling: Styling, simulation, and rendering. **IEEE Transactions on Visualization and Computer Graphics**, IEEE Educational Activities Department, USA, v. 13, n. 2, p. 213–234, mar. 2007. ISSN 1077-2626. Available from Internet: <<https://doi.org/10.1109/TVCG.2007.30>>.

WEI, L. et al. Real-time hair rendering using sequential adversarial networks. In: **Proceedings of the European Conference on Computer Vision (ECCV)**. [S.l.: s.n.], 2018.

XING, X. et al. Real-time rendering of animated hair under dynamic, low-frequency environmental lighting. In: **Proceedings of the 11th ACM SIGGRAPH International Conference on Virtual-Reality Continuum and Its Applications in Industry**. New York, NY, USA: Association for Computing Machinery, 2012. (VRCAI '12), p. 43–46. ISBN 9781450318259. Available from Internet: <<https://doi.org/10.1145/2407516.2407528>>.

YU, X. et al. A framework for rendering complex scattering effects on hair. In: **Proceedings of the ACM SIGGRAPH Symposium on Interactive 3D Graphics and Games**. New York, NY, USA: Association for Computing Machinery, 2012. (I3D '12), p. 111–118. ISBN 9781450311946. Available from Internet: <<https://doi.org/10.1145/2159616.2159635>>.

YUKSEL, C.; KEYSER, J. Deep opacity maps. **Computer Graphics Forum (Proceedings of EUROGRAPHICS 2008)**, v. 27, n. 2, p. 675–680, 2008.

YUKSEL, C.; TARIQ, S. Advanced techniques in real-time hair rendering and simulation. In: **ACM SIGGRAPH 2010 Courses**. New York, NY, USA: Association for Computing Machinery, 2010. (SIGGRAPH '10). ISBN 9781450303958. Available from Internet: <<https://doi.org/10.1145/1837101.1837102>>.

ZINKE, A. et al. Dual scattering approximation for fast multiple scattering in hair. **ACM Trans. Graph.**, Association for Computing Machinery, New York, NY, USA, v. 27, n. 3, p. 1–10, aug. 2008. ISSN 0730-0301. Available from Internet: <<https://doi.org/10.1145/1360612.1360631>>.